Article | Received 11 December 2025; Revised 14 February 2026; Accepted 19 March 2026; Published 26 March 2026
https://doi.org/10.55092/rse20260004

Low-frequency energy harvesting using a counterweighted pendulum for maritime applications

Kacper Wojkowski, Iain Mitchell and Ahmad Serjouei*

Department of Engineering, School of Science and Technology, Nottingham Trent University, Nottingham NG11 8NS, UK

* Correspondence author; E-mail: ahmad.serjouei@ntu.ac.uk.

Highlights:

- Counterweighted pendulum harvester optimized for ultra-low-frequency marine roll.
- Tuneable mass–length–counterweight design achieves compact sub-Hz resonance.
- Stepper-generator architecture provides robust, maintenance-light power generation.
- Prototype delivers 1.55 W at 0.3 Hz, outperforming comparable low-frequency harvesters.

Abstract: This paper presents the design, development, and experimental evaluation of a low-frequency energy harvesting device based on a counterweighted pendulum system. Targeting maritime applications, particularly as an emergency power source for lighting or homing beacons, the device converts mechanical oscillations into electrical energy using a stepper motor, a mechanical motion rectifier, and a flywheel. A key focus is tuning the system for resonance at low excitation frequencies typical of marine environments. Through a series of controlled tests, the system achieved a peak average power output of 1.553 W at 0.3 Hz using a 3.049 kg pendulum at a 25 cm length. Comparative analysis highlights the efficiency gains from tuning pendulum length, mass, and counterweight placement. The device architecture emphasizes low-maintenance operation, passive actuation, and the use of manufacturable, modular components suitable for scalable production and integration into maritime or industrial platforms. These attributes position the system as a sustainable energy-harvesting solution that can complement hybrid power architectures and contribute to circular manufacturing approaches by reducing reliance on disposable batteries in remote systems. The results demonstrate significant improvements over similar harvesting technologies operating at higher frequencies and lay the groundwork for broader deployment in resilient, sustainable marine systems.

Keywords: energy harvesting; counterweighted pendulum; mechanical motion rectifier; stepper generator; low-frequency oscillation; renewable energy

1. Introduction

Access to reliable electrical power is vital for maritime safety and onboard functionality. Small vessels, such as lifeboats, sailboats, autonomous craft, and unpowered utility boats, often operate with

minimal electrical infrastructure due to constraints on space, weight, and cost. This becomes especially critical in emergency scenarios, where essential devices like Emergency Position-Indicating Radio Beacons (EPIRBs), Automatic Identification Systems (AIS), and distress lighting must remain operational for extended periods. Relying solely on stored batteries is risky, particularly for long durations at sea or when pre-departure charging is incomplete. The European Maritime Safety Agency reports over 650 lives lost across 444 marine casualties between 2014 and 2023, underscoring the urgent need for dependable, self-sufficient power solutions [1].

Ocean waves represent an abundant but underutilised source of kinetic energy, with a global estimated potential of approximately 93,000 terawatt-hours (TWh) annually [2]. However, large-scale marine technologies, like oscillating water columns or offshore turbines, are unsuitable for mobile, small-scale applications. Passive systems that harvest energy from a vessel's inherent motion are being actively explored. Yet, piezoelectric and triboelectric solutions suffer from poor durability, low output, or unsuitability in humid, salt-rich environments [3,4]. Micro-scale electret-based generators, which use permanently charged polymer membranes to convert vibration into electricity, have also been investigated. For example, Arakawa *et al.* [5] developed a micro electret membrane harvester producing approximately 6 μW, suitable only for miniature electronics. However, such systems remain impractical for marine environments due to their fragility, low power output, and limited scalability.

In contrast, electromagnetic systems have shown greater practicality at low frequencies. Saha *et al.* [6] showed that compact electromagnetic harvesters can generate several hundred milliwatts from low-frequency human motion, indicating strong potential for low-RPM energy harvesting under marine-like conditions. In recent years, pendulum based harvesters have emerged as particularly promising for extracting energy from low frequency oscillation. A wide ranging review by Chen *et al.* [7] analysed single and double pendulum energy harvesters across electromagnetic, piezoelectric, and triboelectric mechanisms, identifying key design strategies such as dynamic tuning, nonlinearity exploitation, and mechanical rectification to improve harvesting efficiency at ultra low frequencies.

Further studies on cross domain pendulum harvesting reinforce this suitability. For example, pendulum inertial electromagnetic harvesters have been shown to convert irregular, multidirectional human motion into unidirectional high frequency rotation via frequency up conversion, achieving peak power around 54 mW in treadmill tests, demonstrating the robustness of pendulum driven rectification even under noisy excitation inputs [8]. Likewise, pendulum like piezoelectric harvesters have been proposed for low frequency sensor powering, illustrating the broader applicability of pendulum geometries across power scales and environments [9].

Within the marine energy community, pendulum wave energy converters (WECs) have been developed and validated experimentally. Qiu *et al.* [10] conducted tests on a bottom hinged pendulum converter and reported that its energy conversion efficiency depends strongly on hydrodynamic damping and ballast configuration—highlighting the importance of mass distribution and restoring torque in pendulum based devices. These hydrodynamic sensitivities align directly with design parameters such as pendulum length, mass, and counterweight placement, which are tunable in the present study.

A substantial body of recent work demonstrates the viability of pendulum WECs for low-to-moderate sea states. For instance, the Pendulum Wave Energy Converter (PeWEC) developed by Pozzi *et al.* [11], was specifically designed for the comparatively milder but more survivable Mediterranean wave climate. Their mathematical and experimental investigations confirmed that pendulum-based converters maintain

stable and efficient performance across regular and irregular sea states. More advanced architectures include the double mass pendulum (DMP) system proposed by Cai *et al.* [12], which achieves ultra low natural frequencies (0.2–1.4 Hz) through mass-position tuning, frequencies that are otherwise difficult to access in compact devices. Their shake-table and wave-flume experiments demonstrated significant output power and strong scalability potential for low-frequency WEC applications. Additionally, parametrically excited pendulum systems have shown considerable promise. Yurchenko *et al.* [13] demonstrated that parametric excitation can reduce the effective gravitational restoring force on the pendulum, enabling dominant rotational motion without gearboxes and improving power capture efficiency while retaining mechanical simplicity.

Beyond these designs, nonlinear and magnetically assisted pendulum harvesters have been explored. Kuang *et al.* [14] demonstrated a magnetic rolling pendulum system leveraging subharmonic resonance to broaden the operational frequency range. While effective for bandwidth enhancement, such systems involve magnetic tuning and more complex nonlinear dynamics, making them less suitable for passive, low-maintenance maritime deployment. Similarly, Graves *et al.* [15], developed a scalable pendulum-based energy harvester for unmanned surface vehicles. Their system utilized a DC motor and planetary gearbox to convert oscillatory motion into electrical energy and demonstrated promising performance at moderate frequencies. However, it relied on complex gearing and brushed components, which can limit robustness and increase maintenance demands.

More recently, Zhao *et al.* [16] presented a chaotic pendulum based nanogenerator that captures high entropy, broadband wave energy using a non resonant, tower integrated design. Their chaotic pendulum converts disordered wave motion into regular mechanical output, enabling both triboelectric and electromagnetic generation with peak power densities up to 56.7 W/m³·Hz and 192.3 W/m³·Hz. Water tank and open sea trials demonstrated strong potential for powering long endurance unmanned systems. While highly effective for broadband conditions, this architecture is considerably more complex than the passive, tuneable resonant system developed in the present work, which is optimised specifically for ultra low frequency roll and low maintenance maritime deployment.

All marine vessels experience six degrees of motion, namely surge, sway, heave (translation), and roll, pitch, and yaw (rotation), from interactions with waves and environment [17]. Among these, roll motion is particularly promising for passive energy harvesting. Roll typically occurs at low natural frequencies (0.1–0.4 Hz), has comparatively low damping, and often exhibits regular oscillation patterns in small- to mid-size boats [18]. This makes it ideal for coupling with resonant systems like counterweighted pendulums. Additionally, roll motion's amplitude and predictability allow for simpler and more reliable mechanical designs, which is critical in emergency scenarios.

While multi degree of freedom (DOF) tri and double mass pendulums [12,13,19] can achieve low frequency or even length independent behavior, they do so at the cost of additional moving bodies, internal couplings, and nonlinear interactions that complicate sealing, increase wear points, and demand tighter manufacturing tolerances, traits that are undesirable for emergency systems expected to remain idle for long periods and function on demand. In contrast, the present harvester is intentionally simple, compact, and tuneable: by adjusting pendulum length, total mass, and counterweight placement, it attains sub-Hz resonance within a constrained footprint suitable for small craft, while the mechanical motion rectifier plus stepper generator pairing provides low maintenance conversion of bidirectional roll into unidirectional rotation. This system level integration, compact sub-Hz tuning without multi mass

complexity, combined with a passive rectified drivetrain, addresses real installation and reliability constraints encountered in small craft maritime environments.

This study presents a counterweighted pendulum-based energy harvester designed for integration aboard maritime vessels. The system captures roll-induced motion and transforms it into unidirectional rotation via a Mechanical Motion Rectifier (MMR), which then drives a stepper motor operating as a generator. Unlike traditional designs relying on brushed DC motors and planetary gearboxes, this system is simpler and tuned for lower-frequency operation. Key to its performance is tuneability: the pendulum's mass and counterweight position can be adjusted to match sea state or vessel characteristics. From a sustainable manufacturing perspective, the device relies on simple, modular mechanical components that can be produced, repaired, or replaced using standard fabrication processes, enabling long service life and reducing material waste. The scalable architecture of the pendulum–MMR system also allows integration into industrial or maritime platforms where low-frequency ambient motion is available, supporting circular and energy-efficient manufacturing ecosystems. By offering a passive, maintenance-light energy source, the device reduces dependency on disposable batteries, aligning with circular manufacturing principles and promoting more sustainable operational cycles in harsh environments.

2. Experimental methods

2.1. Device concept and operational principle

The energy harvester consists of a counterweighted pendulum mounted within an aluminium frame. Pendulum oscillations, driven by external motion, are converted into continuous unidirectional rotation using an MMR, which subsequently drives a stepper motor generator via a flywheel and gear transmission system.

The MMR, composed of bevel gears and one-way clutches, rectifies bidirectional pendulum motion. A flywheel smooths output and bridges inactive phases near the pendulum’s apex. Power is transmitted through a timing-belt driven planetary gearbox that amplifies RPM to optimize the stepper motor’s voltage output. System tunability is achieved through adjustments to pendulum length, mass, and counterweight position.

2.2. Mechanical architecture

2.2.1. Structural frame

The frame, constructed from 20 mm aluminium extrusions, provides a rigid, corrosion-resistant, and modular base for the system. Its open-cuboidal design (400 mm × 500 mm × 400 mm) offers easy access for component adjustment and testing. Aluminium was selected for its strength-to-weight ratio and suitability for marine environments.

2.2.2. MMR

The MMR converts oscillatory input into unidirectional output using three bevel gears and two one-way clutches. Two input gears (A and B), mounted on the pendulum shaft, alternately engage the output bevel gear depending on swing direction: Gear A engages during clockwise motion, Gear B during counterclockwise motion. The output gear transfers motion at 90° to the pendulum shaft, ensuring

continuous unidirectional rotation suitable for generator input. Diagrams illustrating this configuration are included in Figure 1.

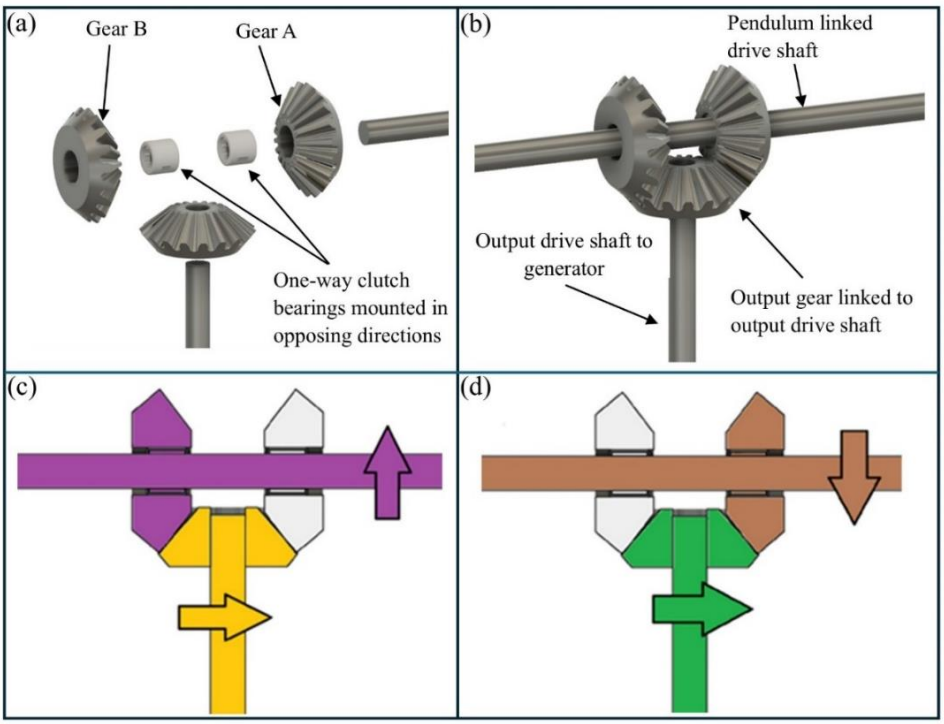

Figure 1. MMR structure and operating principle: **(a)** Disassembled MMR with labelled components; **(b)** Assembled MMR with labelled components; **(c)** Cross-section showing gear B engagement during counter-clockwise pendulum swing; **(d)** Cross-section showing gear A engagement during clockwise pendulum swing.

2.2.3. Flywheel and energy smoothing

A large spur gear mounted on the output shaft serves as a flywheel to smooth energy delivery. It stores kinetic energy during active drive phases and sustains rotation during transitions near the swing apex when the MMR disengages. The flywheel also acts as a rotation amplifier, transmitting power to a smaller spur gear, thus increasing input speed to the generator.

2.2.4. Adjustable counterweighted pendulum

The pendulum is constructed from aluminium extrusions and includes symmetrical arms extending 30 cm above and 25 cm below the pivot. A custom-machined aluminium block joins the arms and incorporates a sliding weight mechanism for counterweight adjustment. This allows tuning of the system's natural frequency by varying both the mass and position of the counterweight and main mass, effectively altering the system's centre of mass and restoring torque.

2.2.5. Generator and transmission assembly

Mechanical output from the MMR is delivered via a 108-tooth flywheel gear to a 36-tooth gear using an HTD 5M timing belt (3:1 ratio), which drives a NEMA 23 planetary gearbox with a 10:1 ratio. This yields a

total mechanical amplification of 30:1 to the stepper motor generator (RS Code: 180-5283), enabling power generation at low pendulum frequencies. The generator and gearbox are rigidly mounted to the frame using 40 mm aluminium struts and a custom mounting plate to minimize vibration and misalignment.

2.3. Oscillating test platform

To simulate wave-induced motion, a single-axis oscillating platform was constructed, capable of ± 20° tilt to reflect typical sea-state roll amplitudes. The platform on which the main device is mounted, measured 45 cm × 65 cm. It was secured 25 cm above a larger steel base by a point of rotation using 40 mm struts. A high-torque Nema 24 stepper motor operating at around 4.2 A and 50 V DC was chosen to withstand the necessary forces. It is controlled by an Arduino microcontroller which then actuates the platform using a crank-arm linkage. The crank arm linkage mounts to the centre of the stepper motor to an anchor point below the base which the device is mounted to. The large stepper motors drive shaft centred 15 cm from the middle of the support beam, raised by 9 cm off the steel base. The anchor point was placed ~2.5 cm from the edge and 5 cm below the oscillating platform. The lengths of the linkage arm were adjusted so that a full rotation of the motor resulted in a ± 20° oscillation. This was measured with a digital level; the final arm lengths were ~12 cm and ~7 cm. The system supports programmable oscillation at 0.1, 0.2, 0.3, and 0.4 Hz, corresponding to sway periods corresponding to sway periods of approximately 10 s, 5 s, 3.33 s, and 2.5 s, respectively, enabling controlled testing of the pendulum system's resonance response. The full assembly is shown in Figure 2.

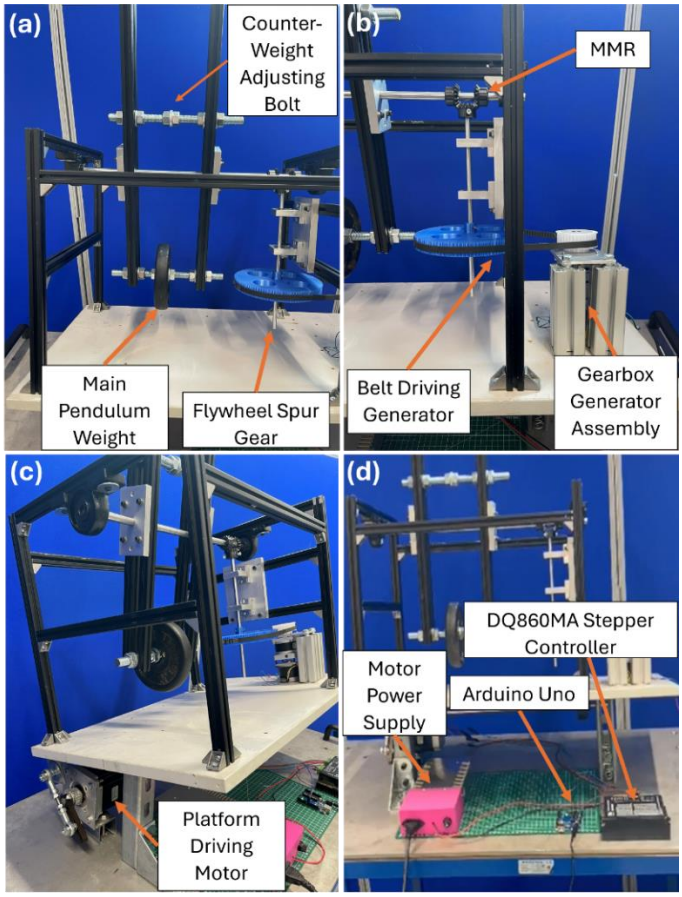

Figure 2. Labelled diagrams of: **(a)** inertial components; **(b)** drive train and generator; **(c)** the platform motor; **(d)** power delivery and control components.

2.4. Data acquisition and processing

Voltage output from the generator coils was measured using a Tektronix TBS2104B 4-channel digital oscilloscope and 10× probes. Measurements were taken across both generator coils under varying frequencies and load conditions. A shunt resistor was used to estimate current and calculate power using:

$$P = \frac{V^2}{R} \quad (1)$$

where V is the combined instantaneous voltage across the resistor and R = 200 Ω. Load selection was based on iterative testing using a variable resistor to balance power output with the electromagnetic drag of the stepper motor. A fixed 200 Ω resistor was ultimately selected as optimal. A schematic of how the two-phase stepper motor generator was tested to measure voltages across shunt resistors is shown in Figure 3.

Waveform data was collected over 6.4 s intervals and exported via Tektronix KickStart 2 software as .CSV files. Post-processing of the collected data included: (i) RMS voltage calculation per coil; (ii) Combined RMS voltage using voltage from coil A (V_1) and voltage from coil B (V_2):

$$V_{RMS_{total}} = \sqrt{{V_1}^2 + {V_2}^2} \quad (2)$$

(iii) Instantaneous and average power computation across the time window; and (iv) Time-resolved plots of RMS voltage and power.

This process enabled quantification of transient and steady-state electrical performance under controlled test conditions.

The probes were connected to the oscilloscope's isolated Bayonet Neill–Concelman (BNC) inputs, and waveform data was recorded at different operating frequencies and load conditions.

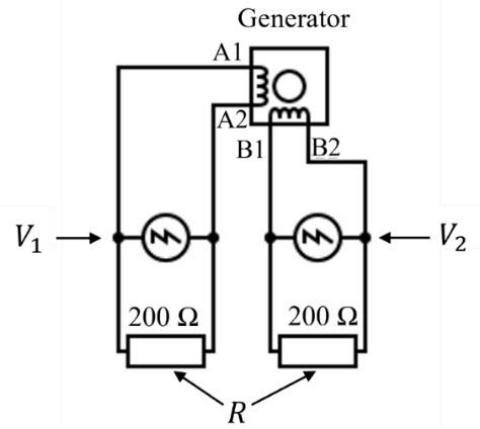

Figure 3. Two-phase stepper motor generator testing schematic (A1 and A2 are coil A connections and B1 and B2 are coil B connections and voltage V_1 and V_2 are voltages for coils A and B, respectively; R is Shunt resistor value).

3. Mathematical modelling

3.1. Pendulum frequency tuning and resonance

The energy harvester's performance depends on how well the movement of the pendulum resonates with the stimulating frequency. Due to the adjustable design, we can tune the pendulums natural frequency

response by adjusting the size and placements of the main and counter-weight masses. This synchronization will amplify energy capture via resonance. The target oscillation frequencies for this device are 0.1 Hz, 0.2 Hz, 0.3 Hz, and 0.4 Hz, corresponding to sway periods of approximately 10 s, 5 s, 3.33 s, and 2.5 s, respectively. The system consists of a main pendulum mass suspended below a pivot, and a movable counterweight mounted above the pivot to modify the system's balance and dynamics.

3.2. Natural frequency of a counterweighted pendulum

For small angular displacements, the pendulum's natural frequency can be approximated using the standard pendulum equation [20]:

$$f = \frac{1}{2\pi} \times \sqrt{\frac{g}{L_{eff}}} \tag{3}$$

where f is the natural frequency (Hz), g is gravitational acceleration (9.81 m/s²) and L_{eff} is the effective length, the vertical distance below the pivot of the system's centre of mass (in metres). This equation shows that a longer effective length results in a lower natural frequency, while a shorter length increases the frequency.

3.3. Influence of mass and position on effective length

In a counterweighted design, L_{eff} depends on both the masses and positions of the main weight and the counterweight. The centre of mass of the system is calculated as:

$$L_{eff} = \frac{m_{arm}d_{arm} + m_{counter}d_{counter} + m_{main}d_{main}}{m} \tag{4}$$

where m_{arm} is mass of the entire arm (kg), $m_{counter}$ is mass of the counterweight (kg), m_{main} is mass of the main weight (kg), d_{arm} is distance of the arm's centre of mass from the pivot (m), above the pivot (so d_{arm} is negative), $d_{counter}$ is distance of the counter weight from the pivot (m), above the pivot (so d_{arm} is negative), d_{main} is distance of the main weight from the pivot (m), below the pivot (so d_{main} is positive).

From this relationship, the following can be conceived: Increasing the mass or distance of the main weight increases L_{eff}, which lowers the frequency; Increasing the mass or height of the counterweight reduces L_{eff}, raising the frequency; Moving the counterweight closer to the pivot or reducing its mass increases L_{eff}, lowering the frequency.

This gives a way to adjust the dynamic response of the pendulum using only mechanical components.

3.4. Mathematically modelled peak performance zones

To estimate the effective lengths, L_{eff}, required to achieve optimal resonance at specific frequencies, we rearrange Equation (1):

$$L_{eff} = \frac{g}{(2\pi f)^2} \tag{5}$$

The L_{eff} values calculated give us an idea of how to load the counterweighted pendulum for the given frequency. These L_{eff} values, given in Table 1, represent the vertical distance from the pivot to the system's centre of mass required to achieve resonance at each frequency.

Table 1. Ideal L_{eff} for target frequencies.

Target Frequency (Hz)	Period (s)	Required L_{eff} (m)
0.1	10.0	2.52
0.2	5.0	0.63
0.3	3.33	0.28
0.4	2.5	0.16

For resonance to effectively enhance power output, the pendulum frequency must closely match the platform oscillation frequency. However, physical constraints such as maximum pendulum length and allowable counterweight travel limit the tuning range.

Using Equation (1), it can be shown that attempting to tune for frequencies above ~0.4 Hz is impractical due to the short pendulum length and mass distribution. Equally achieving resonance at 0.1 Hz is impractical given device size and damping losses to the minimal stimulation.

Hence, the harvester is optimized for the mid-frequency range typical of ocean wave roll motions, balancing mechanical feasibility with energy capture efficiency. This is done by raising the system's centre of mass using a strategically positioned counterweight, to simulate a shorter effective pendulum.

3.5. Design considerations and test setup

The counterweighted pendulum includes an inherent internal bias from its construction. Even with no weights added, the system behaves as if a 0.05 kg counterweight mass is located 15 cm above the pivot. This is represented as the m_{arm} and d_{arm} values in the L_{eff} calculations. This construction bias is always present and is not shown in the results tables for better consistency when comparing data.

Additionally, a 0.549 kg bolt mechanism used to secure weights is treated as a 0.5 kg mass for simplicity, meaning that listed pendulum masses of 0.5 kg, 2 kg, 2.5 kg, and 3 kg correspond to actual values of 0.549 kg, 2.049 kg, 2.549 kg, and 3.049 kg.

Testing was conducted over the target frequency range of 0.1–0.3 Hz. Attempts to reach 0.4 Hz were abandoned due to structural limitations of the oscillating platform. Table 2 lists the variables and their range used in experiments for data collection.

Table 2. List of variables and their ranges used in experiments for data collection.

Variable	Range
Frequency	0.1, 0.2, 0.3
Counter length (cm)	0, 10, 15, 20, 30
Counter mass (Kg)	0, 0.5
Pendulum length (cm)	10, 15, 20, 25
Pendulum Mass (Kg)	2, 2.5, 3

4. Results and discussion

4.1. Influence of pendulum length

The effect of pendulum length on energy harvesting performance was investigated using three lengths (10 cm, 15 cm, and 25 cm) while maintaining a constant pendulum mass of 3 kg. These configurations were tested across several oscillation frequencies, with the objective of identifying resonance and quantifying output power. As shown in Figure 4 (and listed in Table 3), longer pendulums yielded significantly higher output power.

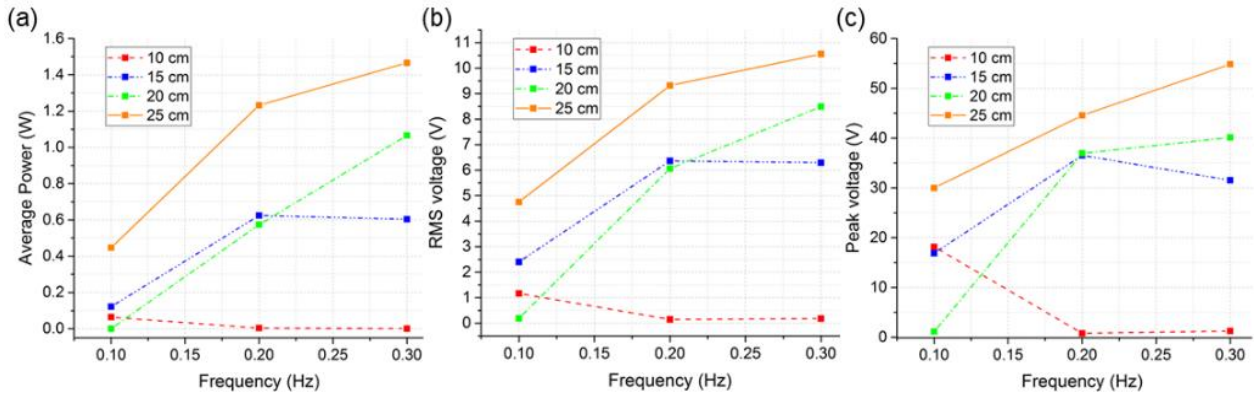

Figure 4. Effect of pendulum length: **(a)** Average power recorded at different 3 kg pendulum lengths with selected frequencies; **(b)** Graph showing the RMS voltage recorded at different 3 kg pendulum lengths with selected frequencies; **(c)** Graph showing the peak voltage recorded at different 3 kg pendulum lengths with selected frequencies.

Table 3. Effect of different pendulum length across frequencies (with construction bias).

Frequency (Hz)	Counter Mass (Kg)	Counter Length (cm)	Pendulum Mass (Kg)	Pendulum Length (cm)	Average Power (W)	RMS (V)	Peak Power (W)	Peak Voltage (V)
0.1	0	0	3	10	0.0643	1.1669	1.6552	18.195
0.1	0	0	3	15	0.1219	2.4021	1.4248	16.881
0.1	0	0	3	20	0.0004	0.1916	0.0064	1.1314
0.1	0	0	3	25	0.4465	4.7542	4.4960	29.987
0.2	0	0	3	10	0.0003	0.1471	0.0032	0.8000
0.2	0	0	3	15	0.6245	6.3641	6.6760	36.540
0.2	0	0	3	20	0.5743	6.0633	6.8240	36.943
0.2	0	0	3	25	1.2316	9.3200	9.9272	44.558
0.3	0	0	3	10	0.0004	0.1778	0.0080	1.2649
0.3	0	0	3	15	0.6040	6.2942	4.9736	31.539
0.3	0	0	3	20	1.0658	8.4932	8.0552	40.138
0.3	0	0	3	25	1.4662	10.545	15.034	54.834

The highest recorded average power output of 1.466 W was obtained using the 25 cm pendulum at 0.3 Hz, indicating operation near the system's natural resonance. In contrast, the 15 cm configuration achieved a maximum average power of 0.624 W at 0.2 Hz, suggesting a resonance point between 0.2 and

0.3 Hz. The 10 cm configuration performed poorly across most frequencies, generating only 0.064 W at 0.1 Hz and negligible power elsewhere. This trend is attributed to increased frictional and stiction losses, which disproportionately affect lower-length configurations with insufficient torque to overcome static resistance. These results confirm that effective pendulum length plays a critical role in tuning the system toward resonance and overcoming internal damping.

The trends in Figure 4 arise from the combined influence of gravitational restoring torque, angular displacement, and the generator's electromechanical loading. Increasing pendulum length lowers the natural frequency, allowing the 25 cm configuration to approach resonance near 0.3 Hz. At resonance, the pendulum experiences larger angular excursions, producing higher rotational velocity at the MMR input. This leads directly to higher RMS and peak voltages and therefore greater average power. In contrast, the 10 cm and 15 cm pendulums possess much higher natural frequencies; at the imposed excitation frequencies (0.1–0.3 Hz), they operate far below resonance, resulting in small angular displacement and insufficient torque to continuously overcome static friction and internal damping within the bearings and rectifier. This produces the "flat" low-power curves observed in Figure 4 for shorter lengths. The much stronger rise in output for the 25 cm pendulum with increasing frequency reflects the system's approach to resonance, where gravitational input and energy transfer efficiency peak.

4.2. Effect of pendulum mass

To isolate the impact of pendulum mass on power output, a fixed pendulum length of 25 cm was used, identified as optimal from Section 4.1. Tests were conducted using masses of 2 kg, 2.5 kg, and 3 kg across oscillation frequencies of 0.1 Hz to 0.3 Hz (see Table 4). As shown in Figure 5, increasing both mass and frequency led to enhanced power generation.

Table 4. Effect of different pendulum mass across frequencies (with construction bias).

Frequency (Hz)	Counter Mass (Kg)	Counter Length (cm)	Pendulum Mass (Kg)	Pendulum Length (cm)	Average Power (W)	RMS (V)	Peak Power (W)	Peak Voltage (V)
0.1	0	0	2	25	0.1566	1.8682	4.0104	28.321
0.1	0	0	2.5	25	0.1845	2.5490	3.9208	28.003
0.1	0	0	3	25	0.4465	4.7543	4.4960	29.987
0.2	0	0	2	25	0.3734	4.5772	4.5200	30.067
0.2	0	0	2.5	25	0.9088	7.9244	7.2520	38.084
0.2	0	0	3	25	1.2316	9.3200	9.9272	44.558
0.3	0	0	2	25	0.7328	6.8294	7.1968	37.939
0.3	0	0	2.5	25	1.3743	9.4338	12.405	49.809
0.3	0	0	3	25	1.4662	10.545	15.034	54.834

At 0.3 Hz, average power rose from 0.733 W (2 kg) to 1.374 W (2.5 kg), then to 1.466 W (3 kg). However, the incremental increase from 2.5 kg to 3 kg was only 0.092 W (6.7%), indicating diminishing returns. At 0.1 Hz, all masses generated similar peak voltages (~28–30 V), Figure 5c, reinforcing that pendulum velocity, rather than mass alone, dictates peak output at lower frequencies.

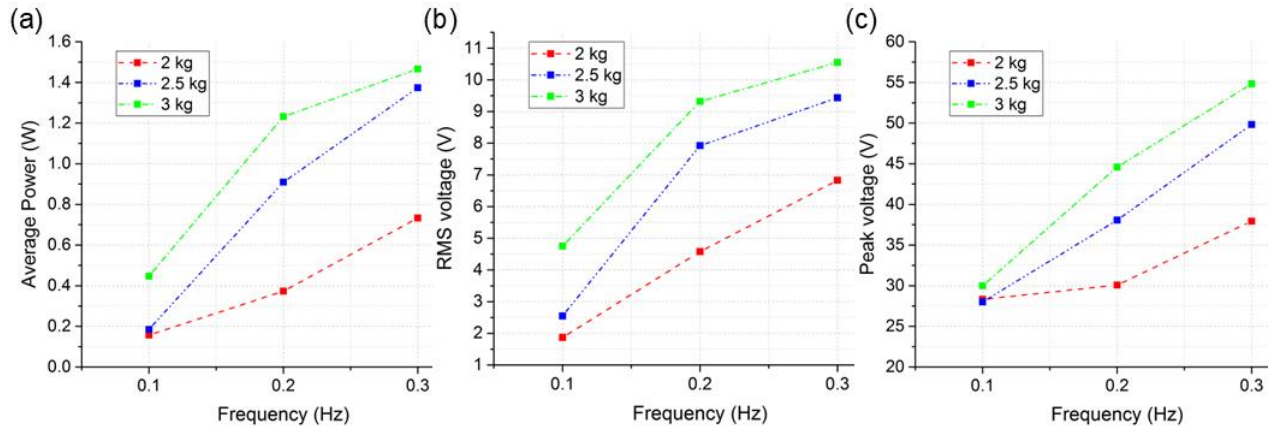

Figure 5. Effect of pendulum mass: **(a)** Average power, **(b)** RMS voltage and **(c)** peak voltage, recorded at different pendulum masses at 25 cm with selected frequencies.

This implies that under reduced frictional losses, lower-mass pendulums may perform more efficiently, particularly at lower frequencies. A potential explanation for this behavior could be due to the lower masses possessing less inertia which needs to be overcome before the pendulum swings in the other direction. These observations suggest that excessive mass may not significantly enhance performance in damping-dominant regimes and highlight the need to optimize pendulum inertia relative to system resistance.

The curves in Figure 5 follow from the interplay between inertia and mechanical losses. As mass increases, the pendulum experiences a larger gravitational torque for a given angle, enabling it to better overcome frictional losses in the MMR and generator. This explains the monotonic rise in RMS voltage and average power from 2 kg to 3 kg at 0.3 Hz. However, because friction scales weakly with mass while inertia scales linearly, the benefit of increasing mass diminishes once the pendulum consistently clears static friction each cycle. This yields the plateau-like trend between 2.5 kg and 3 kg. At lower excitation frequencies (e.g., 0.1 Hz), velocity is limited regardless of mass, which explains the similar peak voltages across masses; output is determined primarily by angular velocity rather than torque. The results show that while added mass improves performance in inertia-limited regimes, excessive mass offers only marginal gains once frictional thresholds are reliably exceeded.

4.3. Effect of counterweight placement

4.3.1. Counterweight effect on 25 cm pendulum

This test examined the effect of positioning a 0.5 kg counterweight above the pivot point on system performance, using the optimal 3 kg, 25 cm configuration. The results are listed in Table 5. Figure 6 shows that most counterweight placements reduced power output, primarily due to raising the center of mass and reducing the effective pendulum length (L_{eff}). This shift likely distanced the system from its resonance frequency (28 cm at 0.3 Hz as per Table 1), and increased the energy required for oscillation.

The observed behavior in Figures 6 and 7 can be interpreted through changes in effective pendulum length (L_{eff}), centre of mass height, and the resulting shift in natural frequency. Counterweights placed higher above the pivot raise the centre of mass, shortening L_{eff} and moving the system away from the resonance frequency identified in Section 4.1. This reduces angular amplitude and thus generator engagement time, leading to lower RMS and peak outputs in most configurations. The exception at 10 cm

arises because, although L_{eff} decreases, the counterweight introduces a favourable redistribution of mass that increases angular sensitivity to small excitation angles, reducing dead zones in the rectifier. This produces a broader effective generation window despite a lower peak voltage. At larger offsets (20–30 cm), the destabilising effect dominates, and the system becomes under-responsive.

A notable exception occurred when the counterweight was placed 10 cm above the pivot. At 0.3 Hz, this configuration generated 1.553 W average power and 11.28 V RMS voltage, surpassing the baseline case (1.466 W and 10.55 V). Calculation of L_{eff} revealed a reduction from 24.36 cm (preload only) to 19.58 cm, moving further from theoretical resonance. However, the increased angular response and reduced "dead zones", regions of low generator engagement, likely allowed more consistent power transfer. Although peak voltage dropped from 54.83 V to 50.08 V (Figure 5c), the pendulum's extended dwell time in the effective generation zone compensated for this reduction.

Table 5. Effect of different counterweight position across frequencies on 25 cm pendulum (with construction bias).

Frequency (Hz)	Counter Mass (Kg)	Counter Length (cm)	Pendulum Mass (Kg)	Pendulum Length (cm)	Average Power (W)	RMS (V)	Peak Power (W)	Peak Voltage (V)
0.1	0	0	3	25	0.4465	4.7543	4.4960	29.987
0.1	0.5	10	3	25	0.1441	1.9217	2.3944	21.883
0.1	0.5	20	3	25	0.1628	2.1324	2.9608	24.334
0.1	0.5	30	3	25	0.3237	4.1916	3.6424	26.990
0.2	0	0	3	25	1.2316	9.3200	9.9272	44.558
0.2	0.5	10	3	25	0.8113	6.1225	10.861	46.606
0.2	0.5	20	3	25	0.5969	6.9771	5.1368	32.052
0.2	0.5	30	3	25	0.7314	6.8995	7.0272	37.489
0.3	0	0	3	25	1.4662	10.545	15.034	54.834
0.3	0.5	10	3	25	1.5529	11.275	12.539	50.078
0.3	0.5	20	3	25	1.2463	9.4244	10.378	45.560
0.3	0.5	30	3	25	1.2196	10.447	9.9472	44.603

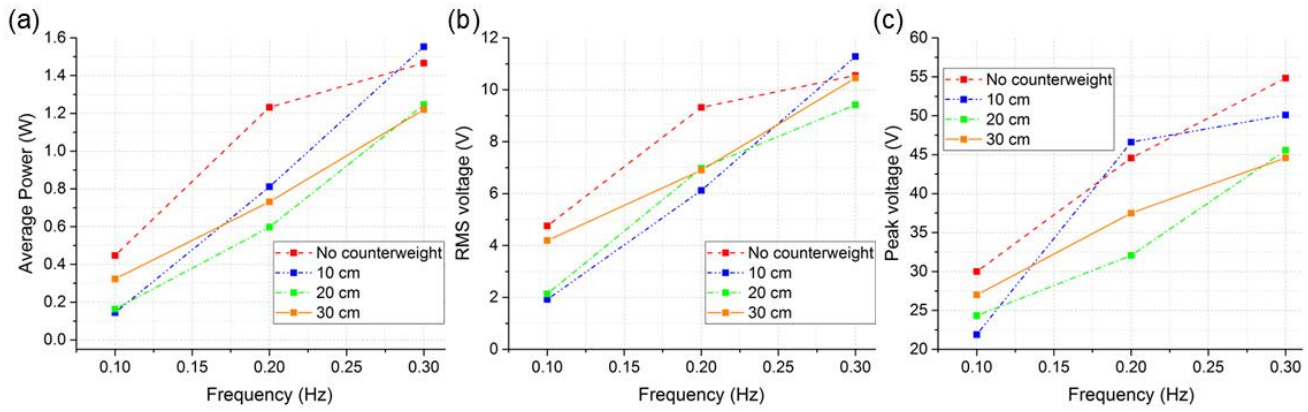

Figure 6. Effect of counterweight placement: **(a)** Average power, **(b)** RMS voltage and **(c)** peak voltage, recorded with different 0.5 kg counterweight positions and 3 kg pendulum at 25 cm across selected frequencies.

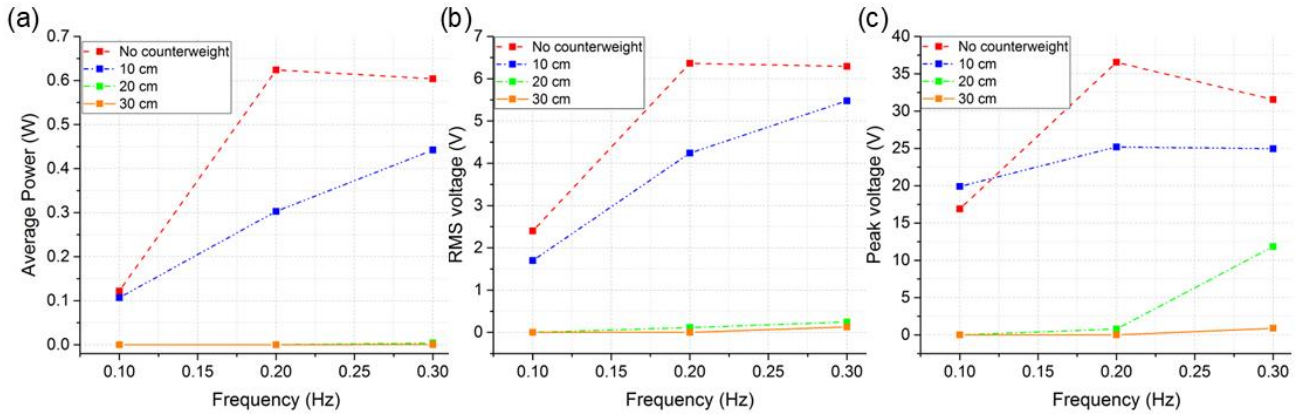

Figure 7. Effect of counterweight placement: **(a)** Average power, **(b)** RMS voltage and **(c)** peak voltage, recorded with different 0.5 kg counterweight positions and 3 kg pendulum at 15 cm across selected frequencies.

4.3.2. Counterweight effect on 15 cm pendulum

Applying a 0.5 kg counterweight to the 15 cm configuration, which already produced limited power, further degraded performance (Figure 7 and Table 6). The raised centre of mass disrupted the already marginal resonance, and in some cases (20 cm and 30 cm placement), no power was recorded below 0.3 Hz. This outcome emphasizes the heightened influence of friction and inertia on short pendulums under counterweighted conditions, reaffirming that optimal counterweighting is configuration-specific.

Table 6. Effect of different counterweight position across frequencies on 15 cm pendulum (with construction bias).

Frequency (Hz)	Counter Mass (Kg)	Counter Length (cm)	Pendulum Mass (Kg)	Pendulum Length (cm)	Average Power (W)	RMS (V)	Peak Power (W)	Peak Voltage (V)
0.1	0	0	3	15	0.1219	2.4021	1.4248	16.881
0.1	0.5	10	3	15	0.1066	1.6995	1.9784	19.892
0.1	0.5	20	3	15	0.0000	0.0000	0.0000	0.0000
0.1	0.5	30	3	15	0.0000	0.0000	0.0000	0.0000
0.2	0	0	3	15	0.6245	6.3641	6.6760	36.540
0.2	0.5	10	3	15	0.3028	4.2412	3.1720	25.187
0.2	0.5	20	3	15	0.0002	0.1162	0.0032	0.8000
0.2	0.5	30	3	15	0.0000	0.0000	0.0000	0.0000
0.3	0	0	3	15	0.6040	6.2942	4.9736	31.539
0.3	0.5	10	3	15	0.4420	5.4780	3.1120	24.948
0.3	0.5	20	3	15	0.0042	0.2443	0.7016	11.846
0.3	0.5	30	3	15	0.0002	0.1294	0.0040	0.8944

4.4. Comparison to literature

The performance of the proposed system was benchmarked against existing low-frequency energy harvesting devices. For instance, Graves *et al.* [15] reported 0.72 W at 1 Hz using a 1.6 kg pendulum.

By comparison, our system achieved 1.553 W at 0.3 Hz using a 3.049 kg mass, more than double the power at one-third the frequency. Table 7 provides a normalized performance comparison.

Table 7. performance comparison of low frequency energy harvesters

Type	Frequency (Hz)	Inertial Mass (Kg)	Power (mW)	Normalised Power (W/Kg)	Reference
Electromagnetic	0.3	3.049	1553	0.51	Current Work
Electrostatic	10	0.7×10^{-3}	6×10^{-3}	8.57	[5]
Electromagnetic	2.5	0.027	1.86	0.07	[6]
Electromagnetic	5.8	0.014	1.31	0.09	[14]
Electromagnetic	1	1.6	720	0.45	[15]

This enhanced performance is attributed to key design elements: a stepper motor optimized for low-speed energy conversion, a dynamically tuned counterweight-pendulum system, and a high-efficiency mechanical motion rectifier. Together, these features enable effective harvesting in low-frequency, high-inertia environments, broadening potential applications to include emergency response systems and infrastructure monitoring in vibration-scarce conditions.

Because the system uses readily manufacturable components and a modular mechanical layout, it is conducive to large-scale production and long-term reuse, key aspects of sustainable and circular manufacturing. Its passive operation and low-maintenance requirements reduce lifecycle energy consumption, supporting the development of more sustainable hybrid power systems for marine and industrial applications.

5. Conclusions and future works

This project successfully developed and tested a fully functional low-frequency energy harvesting system. The rig was designed and machined using precision engineering principles, and components were selected to withstand the intended operating environment. System testing using an oscilloscope and software tools confirmed consistent and repeatable energy generation under various configurations.

The device demonstrated its capability to generate up to 1.553 W of electrical power at just 0.3 Hz using a 3.049 kg counterweighted pendulum which is sufficient to power low-consumption emergency devices such as the Ocean Signal rescueME EPIRB1, which operates at 121.5 MHz on only 50 mW. These results highlight the system's potential in emergency and off-grid applications, particularly aboard marine vessels where external power sources may be unavailable.

The harvester also showed promise as a passive, low-maintenance solution for small-scale energy generation. Future improvements will focus on optimizing the system's mechanical efficiency and energy storage. In particular, redesigning the flywheel to increase its mass and diameter could improve rotational inertia, allowing the generator to maintain output between pendulum swings and reducing output fluctuations.

Additionally, reconfiguring the MMR to align with the pendulum's swing plane may reduce friction and allow for more efficient torque transfer. An alternative design approach could eliminate the flywheel and MMR entirely, instead directly coupling the pendulum to a bidirectional generator (such as a stepper

motor). While this would simplify the mechanical system, it would require more advanced power electronics to rectify and regulate the output.

Another promising feature of this design is its tunability. Test results indicate that adjusting the counterweight position allows for effective resonance tuning, which could be exploited to match specific vibrational environments. For instance, although large commercial ships are designed to reduce roll for cargo stability, they still experience persistent engine-induced vibrations during long voyages. A counterweighted pendulum system tuned to such vibrations could provide a practical, low-maintenance energy source for onboard sensors, safety lights, or control electronics.

Finally, the potential to integrate this technology into hybrid energy architectures, alongside solar panels, waste heat recovery, and other renewable sources, makes it an attractive candidate for advancing energy sustainability in maritime operations.

Data availability statement

The data or datasets that support the findings of this study are available from the corresponding author upon reasonable request.

Declaration of generative AI and AI-assisted technologies

During the preparation of this manuscript, the authors used generative AI tools only to improve language and readability. The authors take full responsibility for the content of the manuscript.

Authors' contribution

Kacper Wojkowski: conceptualization, design, methodology, investigation, data curation and analysis; Iain Mitchell: investigation, and writing—review and editing; Ahmad Serjouei: supervision, writing—original draft, writing—review and editing and validation. All authors have read and agreed to the published version of the manuscript.

Conflicts of interest

The authors declare no competing interests.

References

[1] European Maritime Safety Agency (EMSA). Annual overview of marine casualties and incidents 2024. 2024, pp. 1–66. Available: https://safety4sea.com/wp-content/uploads/2024/12/EMSA-Annual-Overview-of-Marine-Casualties-and-Incidents-2024_11.pdf (accessed on 23 March 2026).

[2] Melikoglu M. Current status and future of ocean energy sources: a global review. *Ocean Eng.* 2018, 148:563–573.

[3] Kim H, Kim J, Kim J. A review of piezoelectric energy harvesting based on vibration. *Int. J. Precis. Eng. Manuf.* 2011, 12(6):1129–1141.

[4] Wang Z, Wang A. On the origin of contact-electrification. *Mater. Today* 2019, 30:34–51.

[5] Arakawa Y, Suzuki Y, Kasagi, N. Micro seismic power generator using electret polymer film. *Proc. PowerMEMS* 2004, 187(190):17.

[6] Saha C, O'Donnell T, Wang N, McCloskey P. Electromagnetic generator for harvesting energy from human motion. *Sens. Actuators, A* 2008, 147(1):248–253.

[7] Chen J, Bao B, Liu J, Wu Y, Wang Q. Pendulum energy harvesters: a review. *Energies* 2022, 15(22):8674.

[8] Wang Z, Hou L, Yao M, Yang T. A pendulum inertial electromagnetic energy harvester for harvesting multiple-source low-frequency human motion energy. *Sci. China Technol. Sci.* 2025, 68(10):2020102.

[9] Lin S, Zhang Z, Zhai S, Zhang L, Gu Y. Construction and performance evaluation of a pendulum-like low-frequency smoothly plucked piezoelectric vibration energy harvester. *IEEE/ASME Trans. Mechatron.* 2025, 30(6):5766–5776.

[10] Qiu S, Ye J, Wang D, Liang F. Experimental study on a pendulum wave energy converter. *China Ocean Eng.* 2013, 27(3):359–368.

[11] Pozzi N, Bracco G, Passione B, Sirigu S, Mattiazzo, G. PeWEC: experimental validation of wave to PTO numerical model. *Ocean Eng.* 2018, 167:114–129.

[12] Cai Q, Zhu S. Applying double-mass pendulum oscillator with tunable ultra-low frequency in wave energy converters. *Appl. Energy* 2021, 298:117228.

[13] Yurchenko D, Alevras P. Parametric pendulum based wave energy converter. *Mech. Syst. Signal Process.* 2018, 99:504–515.

[14] Kuang Y, Hide R, Zhu M. Broadband energy harvesting by nonlinear magnetic rolling pendulum with subharmonic resonance. *Appl. Energy* 2019, 255:113822.

[15] Graves J, Kuang Y, Zhu M. Scalable pendulum energy harvester for unmanned surface vehicles. *Sens. Actuators, A* 2020, 315:112356.

[16] Zhao T, Li Z, Niu B, Xie G, Shangguan L, *et al.* A pendulum-based nanogenerator for high-entropy wave energy harvesting. *Nat. Commun.* 2025, 16(1):5480.

[17] Fossen T. *Handbook of Marine Craft Hydrodynamics and Motion Control*, 1st ed. Chichester: John Wiley & Sons, Inc., 2011.

[18] Deleanu D, Dumitrache C. Controlling the parametric roll of a container ship model by changing the forward velocity. *IOP Conf. Ser.: Mater. Sci. Eng.* 2020, 916(1):12024.

[19] Yurchenko D, Alevras P. Dynamics of the N-pendulum and its application to a wave energy converter concept. *Int. J. Dyn. Control* 2013, 1(4):290–299.

[20] Tolasa D. Theoretical analysis of a simple pendulum experiment. *Int. J. Curr. Res. Sci. Eng. Technol.* 2025, 8:214–218.